Human Umbilical Cord Mesenchymal Stem Cells Grown in 3D Micro-environment Ameliorate Acute Liver Injury by Immunoregulation and Proliferation Promotion

Junhong Zhang
East China University of Science and Technology
Junqi Zhou
East China University of Science and Technology
Yan Peng
East China University of Science and Technology
Ali Mohsin
East China University of Science and Technology
Yanxia Luo
East China University of Science and Technology
Yingpng Zhuang
East China University of Science and Technology
Meijin Guo (guo_mj@ecust.edu.cn)
East China University of Science and Technology https://orcid.org/0000-0002-3171-4802

Research Article

Keywords: Human cord mesenchymal stem cells, 3 D culture, Cell therapy, Inflammatory cytokines, Macrophages, Acute liver injury

Posted Date: January 31st, 2022

DOI: https://doi.org/10.21203/rs.3.rs-1298680/v1

Abstract

Background

Mesenchymal stem cells (MSCs) have been widely used for inflammatory diseases like acute liver injury (ALI) and COVID-19 diseases. However, most MSCs instead of the cell-matrix are cultured in 2 D plates, resulting in degeneration of some key functions along with a limited understanding of the immune response in tissue repairing. Herein, we obtained the human umbilical cord MSCs grown on microcarriers in 3 D suspension culture (3 D hUCMSCs) that proved more appreciative than 2 D hUCMSCs for the ALI therapy.

Methods

hUCMSCs were isolated and respectively cultured in 2 D plates and 3 D microcarriers *in vitro*, and acute liver injury model in mice was used to evaluate tissue repairing ability of the transplanted hUCMSCs. Nitric oxide production, cell proliferation and the relative protein expression level were comprehensively evaluated. Besides, the cytokine expression level in the of serum mice was detected by quantitative RT-PCR and cytokine antibody chip.

Results

When transplanted with 3 D hUCMSCs in ALI mice, the injured liver tissues have a significantly-increased histological scores and enhanced animal's body/liver weight, superior to the 2 D hUCMSCs and control group. Pro-inflammatory cytokines (IL-6, IL-1β, IL-17, IL-22 and TNF-α), apoptosis promoter IFN-g, and NO production declined when transplanted with 3D hUCMSCs compared to the control group. Besides, anti-inflammatory cytokines (IL-10) was up-regulated.

Conclusion

Both the 3 D hUCMSCs and the conditioned medium were more favorable for the therapy of acute liver injury (ALI). Triple regulatory roles of the 3 D hUCMSCs include the effective promotion of M1/M2 macrophage switch through increased secreting of anti-inflammatory cytokines, ameliorating proliferation and NO downregulation of macrophage. A balance of these cytokines in the conditioned medium of 3 D hUCMSCs played a key role in ALI repairing. It was proven that the 3 D hUCMSCs could trigger the mitogen-activated protein kinases (MAPKs) and STAT3 signaling pathways. Conclusively, the revelation of the superior moderating effect of 3 D hUCMSCs and possible regulatory mechanisms will improve the clinical efficacy of stem cell therapy for inflammatory and immunological diseases.

Introduction

Acute liver injury (ALI) is one of the most important causes of mortality worldwide, which usually results in a rapid loss of hepatic function. ALI is associated with an adaptive inflammation response triggered by noxious stimuli, such as infection[1] and chemicals [2]. Macrophages, being the main inflammation-mediated cells, release various inflammatory cytokines such as tumor necrosis factor α (TNF-α), interleukin-6 (IL-6), interleukin-1β (IL-1β)[3, 4], and other inflammatory mediators upon activation by bacterial[5] or virus products [6]. Overexpression of these factors usually leads to a wide range of progressive diseases, including cancer, neurological disease, metabolic disorders and acute tissue injury[7–11]. Thus, suppressing the overexpression of inflammatory cytokines could be a robust tool to ameliorate ALI.

Mesenchymal stem cells (MSCs) are considered as the most important members of stem cell family and found in many tissues, such as bone marrow[12, 13], fat[14, 15], and umbilical cord [16]. Above all, one of the most intriguing biological characteristics of MSCs is their immunomodulatory property, which lays the therapeutic basis of MSCs for inflammatory diseases like autoimmune[17] and COVID-19 diseases [18, 19]. The induction of tissue regeneration after MSCs administration was initially believed that the regeneration occurred upon MSCs-migration and differentiation into the damaged populations[20, 21]. Although MSCs could transdifferentiate functional cells [22], increasing evidence gradually indicates that the specific differentiation of MSCs in damaged tissues is only partly responsible for the disease treatments. Moreover, the paracrine effects act as an alternative strategy. However, most of the conclusion is based on the fact that the MSCs are cultured in 2 D plates *in vitro*, which disregard the complexity of interactions seen *in vivo*. Essentially, in 2D, cells have more surface area to contact with the culture plate and media than with other cells [2], forcing them into a polarization that fails to reflect physiological conditions. This probably results in the degeneration of some key functions and limits the understanding of the immune response in tissue repairing[23, 24]. Thus, it is very necessary to explore a more realistic model like a three-dimensional (3D) culture system, where the cells are grown on a scaffold-based substrate that maximally mimics the extracellular matrix. Morphology, gene expression patterns, cell cycle and proliferation is much closer to physiological conditions.

To this end, herein, we obtained the human umbilical cord MSCs cultured in 3 D microcarriers (3 D hUCMSCs, Scheme 1) and provided the evidence that both the 3 D hUCMSCs and the conditioned medium were more favorable for the therapy of acute liver injury (ALI). Nitric oxide production, cell proliferation, inflammatory cytokines/mRNA expression were comprehensively evaluated. In addition, the change of phosphorylation level of extracellular signal-regulated kinases (ERK), c-Jun N-terminal kinases (JNK), the p38 and STAT3 were assessed to reveal the possible signaling pathways. Consequently, we demonstrated the 3 D hUCMSCs acts as a promising modulator of immune activation, cell proliferation and apoptosis, which suppresses ALI in mice by MAPKs and STAT3 signaling pathways. In short, we believe such a disclosure will bring new hope to patients to cure inflammatory and immunologically mediated diseases.

Materials And Methods

Macrophage Inflammation Model in vitro

RAW 264.7 murine macrophage-like cell line was purchased from the Stem Cell Bank, Chinese Academy of Sciences (Shanghai, China). Cells were cultured in petri dishes (Thermo Fisher Scientific, LabServ, China) using Dulbecco's modified Eagle medium with high glucose (H-DMEM, Gibco, USA), supplemented with 10% heat-inactivated FBS and 100 U/mL penicillin/streptomycin in a humidified air with 5% CO_2 at 37 ℃. The medium was replaced after every 2 days until cells reached 70-80% confluency. An inflammatory model *in vitro* was set up by using lipopolysaccharide (LPS, Merck KGaA, Darmstadt, Germany) to induce RAW 264.7 cells at a concentration of 100 ng/mL (denoted as LPS group).

Culture of hUCMSCs

For 2 D culture, the hUCMSCs were seeded at a density of 5×10^4 cells / mL in a T-75 cell culture flask (Scheme 1) and the medium was replaced every three days. hUCMSCs on the third passage (P3) were adopted for the subsequent experiments[25]. All the numbers and diameter of cells were counted by the automatic counting cell analyzer (CountStar®Regel S3, Ruiyu, China).

For 3 D suspension culture, 1.5 L bioreactors (Guoqiang, China) was used in this study, equipped with dissolved oxygen (DO) probe (Mettler, Toledo) and a pH probe (Mettler, Toledo). The vessels were filled with α-MEM medium and 10% FBS (600 mL), hUCMSCs (1.35×10^5 cells/mL) and Cytodex3 microcarrier (1.8 g, 10 cells/bead). The cells were then inoculated at 37 ℃ with air and 40% DO by bottomspace gassing. The reactors was agitated at 55 rpm for 120 hours to provide the 3 D suspension cultured cells.

Phenotypic Analysis

The P3 hUCMSCs were stained with fluorescent-labeled monoclonal antibodies, including positive markers (APC CD105, FITC CD73 and FITC CD90) and negative ones (FITC CD34, FITC CD45 and FITC HLA-DR). All the markers were purchased from BD Biosciences (USA). IgG was used as an isotype control and cultured under the same condition. The stained cells were sorted into defined populations using fluorescent-activated cell sorting (FACS, Beckman Coulter, CA, USA) to produce a pure population with the appropriate cell marker profile.

Multilineage Differentiation Assays

Adipogenesis. Cells were seeded in 6-well plates at 2.0×10^5 per well and cultured in the presence of adipogenic supplements, consisting of α-MEM, 10% FBS, dexamethasone (1 μM), insulin (10 μg/ mL), L-ascorbic acid 2-phospate (100 μg/mL), 3-isobutyl-1-methyl-xantine (0.5 mM) and indomethacin (20 uM). On day 14, cells were stained with oil red O (Merck KGaA, Germany) at room temperature for 15 minutes, and the cells were visualized under Invitrogen EVOS FL Auto Cell Imaging System.

Osteogenesis. Cells were seeded in 6-well plates at 2.0×10^5 per well and cultured in growth medium to 80-90% confluency. After that, the medium was replaced with osteogenic induction medium, consisting of H-DMEM medium, L-ascorbic acid 2-phospate (50 μg/mL), sodium β-glycerophosphate (10 mM) and

dexamethasone (100 nM). Moreover, the fresh differentiation medium was replaced every 2-3 days for three weeks. Then the cells were fixed in 4% paraformaldehyde for 30 min at 4 ℃ and the calcium nodules were stained by 0.1% Alizarin Red at 37 ℃ for 30 minutes.

Preparation of Conditioned Medium Derived from hUCMSCs

Six-well transwell co-culture system (Corning, USA) with 8 μm pore filters was used to co-culture RAW 264.7 cells and the hUCMSCs, where RAW-264.7 cells (1.0×10^6) and hUCMSCs (1.0×10^5) were seeded into the upper and lower units of the chamber, respectively. The control group was added only with RAW 264.7 cells (1.0×10^6) to the upper chamber. When the hUCMSCs reached 8090% confluency, they were washed three times with PBS and the medium was replaced with serum-free α-MEM medium. After further culturing for 48 h, the conditioned medium (2 D hUCMSCs©) was collected by centrifuge (2000 g for 10 min at 4 ℃) and stored at -80°C until usage. A similar method was used to obtain 3 D hUCMSCs©.

Cell Viability Assay

Cell viability was tested using MTT assay. Firstly, RAW 264.7 cells were seeded in a 96-well plate at a density of 1.0×10^4 cells per well. After incubation for 12 h to allow cells to attach on the wall, the growth medium was removed and the cells were washed 3 times with PBS. Then fresh growth medium and the conditioned medium were added. After further culturing for 24 h, MTT (5 mg/mL, 20 μL) was added and incubated for 4 h at 37 ℃ in a humidified atmosphere with 5% CO_2. MTT was removed and dimethyl sulfoxide (150 μL) was added to dissolve the formazan crystals. The absorbance of colored solution was recorded at 570 nm to calculate the cell viability using a standard method described in the previous report [26].

Cell Apoptosis Assay

Cell apoptosis of RAW 264.7 cells was conducted by flow cytometry according to the manufacturer's instructions of Annexin V-FITC Apoptosis Detection Kit (Dojindo, Tokyo, Japan). RAW 264.7 cells were firstly seeded in a 6-well plate (5.0×10^5 cells per well). After 24 h incubation, the cells were harvested and washed twice with iced PBS. After removing supernatants, the cells were further treated with trypsin for the appropriate time and terminated with the culture medium. Cells were pelleted by centrifugation (1000 rpm, 3 min) and then washed twice. 10X diluted Annexin V Solution was added to re-suspend the cells (cell concentration of 1.0×10^6 cells/mL). Annexin V (5 μL), FITC conjugate and PI solution (5 μL) were respectively added to cell suspension (100 μL) and then the mixed solution was incubated for 15 min free of light. Further dilution using Annexin V solution (400 μL) was required before flow cytometry analysis (Accuri C6,BD Biosciences, USA).

Measurement of Nitric Oxide (NO) Production

RAW 264.7 cells were seeded in 96-well culture plates and incubated for 24 h, then the nitric oxide (NO) concentration in the supernatants of cultured RAW 264.7 cells was measured using a NO assay kit

(Beyotime Institute of Biotechnology, China). The concentration of NO was obtained by reading the absorbance value at 540 nm, where sodium nitrite ($NaNO_2$) was used as an external standard.

Total RNA Extraction and Quantitative RT-PCR Analysis

Total RNA was extracted from cells using a Total RNA Kit (Invitrogen™ TRIzol™, Thermo, USA) according to the manufacturer's instructions. Then cDNA was synthesized with PrimeScript™ RT reagent Kit (Takara, Japan). Real-time PCR was performed with SYBR Premix Ex Taq™ II (Tli RNaseH Plus) Kit (TAKARA, Japan) in the CFX96 touch qPCR system (Bio-Rad, USA). The primer sense and antisense sequences are listed in Table 1. The $2^{-\Delta\Delta Cq}$ method was used to calculate the relative expression level for each gene [27] and normalized to the internal control Housekeeping β-actin gene.

Enzyme-linked Immunosorbent Assay (ELISA)

The concentration of IL-6 was measured via a mouse IL-6 ELISA Kit (R&D Systems, Minneapolis, MN, USA) in the supernatants obtained from RAW 264.7 cells. Absorbance at 450 nm was read on a microplate reader (BioTek, Winooski, Vermont, USA). All the experiments were performed in triplicate and the average value was used to minimize errors. Following the similar method, the concentrations of other cytokines were respectively evaluated.

Western Blotting Analysis

The cytoplasmic protein of RAW 264.7 cells was extracted using a Cytoplasmic Protein Extraction Kit (Beyotime, China). After the extraction, the protein concentrations were determined by Bicinchoninic acid Protein Assay. Then western blot analysis was carried out by applying polyclonal rabbit antibodies such as Erk MAPK, phospho-Erk MAPK, p38 MAPK, phospho-38 MAPK, JNK MAPK, phospho-JNK MAPK, STAT3, phospho-STAT3 and β-actin antibodies. All these antibodies were purchased from Cell Signaling Technology Inc (MA, USA). The secondary antibodies were bought from Signalway Antibody (Signalway Antibody LLC, USA). Protein bands were separated by SDS-polyacrylamide gel electrophoresis (SDS-Page), and the SDS-Page was electroblotted onto PVDF membranes (GE Healthcare, Chicago, IL, USA) and visualized by ECL detection kits (Beyotime, China). Western blot quantification was achieved with Image J software.

ALI Mice Model

Male BLAB-c mice with a bodyweight of ~ 20 g (x5 per group) were employed and the acute liver injury mice model was established by continuously CCl_4 injection via tail vein. The serum ALT and AST levels in the CCl_4-induced mice were assessed to ensure the ALI mice model. After induction for 24 h, the hUCMSCs or the conditioned medium was transplanted into the ALI mice by tail vein. mRNA or cytokines in serum were respectively assessed according to the aforementioned methods.

Statistical Analysis

All data are representative experiments performed in three independent experiments. Data were expressed as mean value ± standard deviation (SD). The statistical significance of the mean values was compared

by one-way *ANOVA* (analysis of variance) and Student's t-test using GraphPad Prism version 8.0.2 software (GraphPad Software Inc., San Diego, USA). *p < 0.05 *vs.* control group, **p < 0.01 *vs.* control group, ***p < 0.001 *vs.* control group; ##p < 0.01, ###p < 0.001 *vs.* control group.

Results

3 D hUCMSCs Attenuates Acute Liver Injury

hUCMSCs were obtained from the human umbilical cord using the enzymatic digestion method [28]. The passage 3 (P3) hUCMSCs were selected for expansion culture due to the inheritance of characteristic stem cell morphology and excellent proliferation potential (Fig. S1). To better mimic the matrix environments *in vivo*, 3 D culture systems *in vitro* (Scheme 1) were explored to incubate the hUCMSCs on the commercialized microcarriers (Cytodex3, images of the scanning electron microscope, please see Fig. S2) in 1.5 L bioreactors. As shown in Fig. 1, the P3 hUCMSCs cultured on the spherical cytodex3 (3 D hUCMSCs) exhibited fusiform or spindle shapes despite of the co-existence of spherical cells (day 1). On day 5, most of the expanded cells displayed homogeneous shapes and then radially arranged and aggregated in the microcarriers. Within the first three days, the 3D hUCMSCs shared a similar proliferation rate with 2D hUCMSCs. For example, On the 3rd day, the cells proliferated to 8.23-fold in 2D and 9.35-fold in 3D Cytodex3 relative to the first day. However, a significant difference was observed once extending to 5 days, when the 3 D hUCMSCs persisted proliferating on spherical Cytodex3 scaffolds to 25.89-fold increment while the cells cultured in 2D decreased to 7.86-fold (Fig. S3). Phenotypic analysis by standard flow cytometry (Fig. 1C) demonstrated that the amplified 3 D hUCMSCs were positive to the specific markers (FITC CD90, APC CD105 and FITC CD73) [29] and negative for a series of surface antigens (FITC CD14, CD19, CD34, CD45 and HLA-DR). Multipotential differentiation evaluation showed that the cells could differentiate into osteocytes, adipocytes and cartilage. These results confirm that the 3 D hUCMSCs used in this study possessed stem cells' typical phenotypes and multipotential characteristics.

ALI mice model [30] was successfully fabricated by consecutive injection with CCl_4. As presented in Fig. 2, the ALT and AST levels were significantly boosted after 24 hours of incubation with CCL_4. The time course of the hepatoprotective effect of the hUCMSCs against CCl_4-induced acute liver injury (ALI) was assessed by evaluating the levels of serum ALT and AST in ALI mice. Compared with the control group, where equivalent PBS buffer as a vehicle, the ALI mice transplanted with the hUCMSCs displayed significantly attenuated serum ALT and AST levels. Especially, the mice transplanted with the 3D hUCMSCs had the lowest serum ALT and AST levels (176.54 and 833.88 U/mL). Additionally, histological examination revealed mild liver injury with cellular necrosis around the blood vessels as early as 12 h. More severe liver injury was observed at 24 h, seen as large areas of extensive cellular necrosis with loss of hepatic architecture and inflammatory cell infiltration around the blood vessels (Fig. 2B & Fig. S4). Interestingly, when transplanted with the 3 D hUCMSCs, a significantly-decreased liver injury were observed with a histological scores of 0.77, 2.52, 3.20, 2.02 and 1.79 respectively (0, 12, 24 36 and 48 h, all P < 0.05 or 0.01), superior than the control group (1.38, 4.59, 5.21, 4.43 and 3.51) and even the 2 D

hUCMSCs (0.99, 3.20, 4.29, 3.38 and 2.60). The animal's body/liver weight showed time-dependent changes with the post-time of hUCMSCs treatment (Fig. 2E&2F). After 1 day post-transplantation, there was an apparent decrease in weight, while the 3 D hUCMSCs group exhibited a slight increase of body/liver weight compared to 2 D hUCMSCs groups.

3D hUCMSCs Altered Liver Responses to Damage through Paracrine Effects

Stem cell application in ALI treatment is attractive, and there are two possible mechanisms responsible for tissue repairing. One is that the liver was repaired through stem cell proliferation and transdifferentiated into hepatocytes. Recent studies further indicate a substantial role for paracrine effects in delivering overall benefits. The activation of liver macrophages into the inflammatory (M1-like) and anti-inflammatory (M2-like) macrophages are usually associated with liver damage. To know the role of paracrine effects on liver repairing in ALI mice, a macrophage-like cell line RAW 264.7 cells was induced with LPS to provide the desired inflammation model *in vitro*. Further, it was then co-cultured with the hUCMSCs by transwell assay, where the hucMSCs were cultured in the lower compartment and the LPS induced RAW 264.7 cells in the upper compartment and were separated by a porous membrane. Conditioned medium derived from the coculture systems were collected by centrifugation, and the medium from 2 D hUCMSCs and 3 D hUCMSCs were denoted as 2 D hUCMSCs© and 3D hUCMSCs©, respectively. Interestingly, we found both 3D hUCMSCs© and 2D hUCMSCs© could relieve the liver injury with a histological score of 0.71, 2.81, 3.02, 2.23 and 1.59 *vs.* 1.25, 3.25, 4.15, 3.5 and 2.65, closer to that of the pertinent hUCMSCs (Fig. 2D and Fig. S5). To learn more about the hUCMSCs on the inflammatory response, we first evaluated the cytotoxicity of the medium *in vitro*. As shown in Fig. 3A, the viability of RAW 264.7 cells increased to 112% when treated with 3D hUCMSCs© ($p < 0.001$), indicating that the medium not only had no significant cytotoxicity to RAW 264.7 cells but also promoted the proliferation of macrophages. Furthermore, apoptosis was detected by flow cytometry (Fig. 3B&E), and the results showed that RAW 264.7 cells mainly displayed late-apoptosis. Surprisingly, the percentage of late-apoptosis cells in the 3D hUCMSCs© group dropped to 4.10%, lower than control group (7.39%) and even 2D hUCMSCs© (5.91%) group. In addition, the AnnexinV/PI double staining suggests that the 3D hUCMSCs© also increased the survival proportion of the RAW 264.7 cells, supporting the result of cell viability analysis. For example, the survival proportion increased to 91.4% from 89.3%. Such response elucidates that the 3D hUCMSCs© could help relieve the late apoptosis of macrophages and enhance the survival proportion, probably due to the cytoprotective effect [31]. Nitric oxide (NO) and inducible NO synthase (iNOS) is usually associated with inflammation, which generally participated in various diseases, including sepsis[32], cancer[33], neurodegeneration[34], and various types of pain [35]. In our experiments *in vitro*, the LPS stimulated RAW 264.7 cells strongly up-regulated the NO production (from 1.48 to 20.9 μM) [36] and significantly enhanced the iNOS mRNA expression level (rises to 7.42 times). However, the NO production and the iNOS mRNA expression were suppressed (Fig. 3C&D) once co-cultured with the 3D hUCMSCs©.

3 D hUCMSCs Impeded the Expression of Pro-inflammatory Cytokines and Up-regulated the Anti-inflammatory Cytokines

To learn more about the therapeutic effect between hUCMSCs and recipient mice hosts, we measured the changes in the serum levels of cytokines and the related messenger RNA (mRNA) changes using cytokines arrays. Cytokine storms were suppressed in the both transplantation group at day 3. In the transplantation group, 9 cytokines (IL-1β, IL-6, IL-10, IL-17, IL-17F, IL-22, IL-28, TGFb1 and TNF-α) showed significant changes (Table 1), suggesting a disparity in the liver responses to damage between the two groups. From a functional perspective, most of the cytokines are related to immunoregulation, signal transduction and promotion/cell death. As a whole, pro-inflammatory cytokines (IL-6, IL-1β, IL-17, IL-22 and TNF-α) and apoptosis promoter IFNg also declined when transplanted 3D hUCMSCs compared to the control group (Fig. 3N). Differently, anti-inflammatory cytokines (IL-10) was up-regulated (Fig. 3M). For convenience, we also evaluate the cytokines change in the conditioned medium from the co-culture of RAW 264.7 cells and hUCMSCs. A similar cytokines change was observed, and the marker related with M_2-like macrophages (Arg-1, CD206 and CD36) were up-regulated when transplanted with 3 D hUCMSCs (Fig. 3F-3H). While the levels of IL-6, IL-1β and TNF-α, produced by the M_1-like macrophages were decreased (Fig. 3I-3K). This result suggested that the 3 D hUCMSCs may be more favorable for M_1/M_2 macrophage switch.

Table 1
Changes of 18 cytokines levels in serum measured by cytokine arrays. Serum was collected on day 3 after the ALI mice were injected with PBS buffer or the hUCMSCs. The value in brackets means cytokines level on day 5.

Cytokines (pg/ml)	PBS	2D hUCMSCs	3D hUCMSCs
IL-1β	35.4(25.9)	31.7(25.9)	21.2(14.3)
IL-2	5.5(3.5)	3.1(3.6)	4.1(0.0)
IL-4	7.1(4.1)	5.4(4.7)	5.0(5.2)
IL-5	617.7(545.5)	431.4(374.0)	401.5(240.6)
IL-6	398.0(361.1)	127.6(94.0)	24.2(14.4)
IL-10	992.0(699.9)	1,316.7(940.4)	1,668.6(1155.2)
IL-12p70	72.6(60.8)	69.1(50.9)	63.7(37.1)
IL-13	57.0(53.4)	75.5(54.7)	43.1(34.8)
IL-17	41.2(13.9)	41.2(3.9)	35.6(2.3)
IL-17F	0.0(0.0)	20.1(11.0)	78.1(44.2)
IL-21	0.0(0.0)	0.0(0.0)	0.0(0.0)
IL-22	24.8(0.0)	109.8(42.0)	232.6(237.9)
IL-23	1,839.1(1517.1)	1,724.5(1586.3)	1,522.6(1569.6)
IL-28	1,149.0(752.7)	1152.4(849.0)	670.9(629.7)
IFNg	3,034.2(1811.0)	3563.4(1,320.0)	873.3(685.8)
MIP-3a	32.3(29.1)	16.8(15.9)	62.1(48.1)
TGFb1	27260.9(12415.1)	12879.1(12152.5)	12,260.9(10999.7)
TNF-α	781.4(187.4)	277.5(255.4)	187.4(154.4)

3D hUCMSCs Increase STAT3 Activation in RAW 264.7 Cells Stimulated with LPS

IL-6 exerts its effects by the interaction with IL-6 receptors [37], which produces conformational changes in the gp130 subunit and activates the signal transducer and activator of transcription 3 (STAT3) via Janus kinases (JAKs). The dysregulation of STAT3 activation has been associated with the pathogenesis of inflammatory diseases [38]. Based on these facts, we hypothesize that hUCMSCs persistently regulated the expression of IL-6 in RAW 264.7 cells and probably stimulated the inflammatory responses of macrophages by inducing the phosphorylation of STAT3. In this study, we found decreased STAT3

protein kinases expression in the 3D hUCMSCs group, in which the declined IL-6 strongly inhibited the activation of STAT3 and the phosphorylation level (Fig. 4A).

3 D hUCMSCs Decrease ERK, p38, and JNK Activation in RAW264.7 Cells Stimulated with LPS

In the ALI model, the macrophages after interaction with the membrane receptors CD14 and Toll-like receptor (TLR)-4, lead to the generation of cytokines such as TNF-α, IL-1β and IL-6 [21]. The signaling pathways in the cell surface are usually mediated by the molecules of mitogen-activated protein kinase (MAPK) family, including ERK, p38 and JNK. To assess whether hUCMSCs interfere with the MAPK signaling cascade, we tested the phosphorylation level of ERK, p38 and JNK of the inflammatory macrophages. Results showed these phosphorylation levels were obviously lower in the presence of 3 D hUCMSCs than in the control sample. Moreover, a significant change was observed in p38 after introducing the hUCMSCs (Fig. 4B&C).

Discussion

Triple Regulatory Roles of the 3 D hUCMSCs on Acute Liver Injury

Macrophages play pivotal roles in maintaining hepatic homeostasis and are closely associated with many liver diseases [21, 22]. Differential expression is now used to identify the heterogeneous macrophage subsets responsible for ALI resolution [22–25]. Regulation of phenotypic switch from M_1 to M_2-like macrophages provides a promising therapeutic intervention for treating the liver injury. Recently, mesenchymal stem cells (MSCs) have been considered the most important members of the stem cell family and found in many tissues, such as bone marrow, fat, and umbilical cord [16]. Above all, one of the most intriguing biological characteristics of MSCs is their immunomodulatory property, widely used for inflammatory diseases like ALI and COVID-19 diseases [18]. However, most MSCs are cultured in 2 D plates instead of the cell matrix-like 3 D environments, resulting in the degradation of some key functions and response sensitivity. Thus, the understanding of the immune response of MSCs *in vivo* was largely limited. Herein, we obtained the human umbilical cord mesenchymal stem cell cultured in 3 D microcarriers (3 D hUCMSCs) and provided the evidence that the 3 D hUCMSCs were more favorable to the MSCs therapy for ALI. Compared to 2 D hUCMSCs, upon liver injury, the ratio of M_1/M_2 like macrophages were remarkably decreased after hUCMSCs transplantation. A similar result was achieved when injected with equal amounts of the conditioned medium [39]. All these indicated the secretions or exosomes of 3 D hUCMSCs would be more favorable for the effective promotion of M_1/M_2 like macrophage switch with an ALI relieving cytokines pattern. Cytokines array or the Elisa data reveal the markedly-shrunk pro-inflammatory cytokines (such as IL-6, IL-1β, IL-17F, IL-22 and TNF-α) and enhanced IL-10 expression level once treated with 3 D hUCMSCs. Besides, in response to LPS stimulation, RAW264.7 produce NO by the enzyme iNOS [40]. The expression of iNOS is very important as a

microbicide, antiviral, antiparasitic and antitumoral molecule. However, the aberrant upregulation of this enzyme is associated with various diseases, including autoimmune disease [41]. In our experiments, stimulation with LPS-stimulated upregulation of iNOS in RAW264.7 cells, and the conditioned medium prevented the upregulation of these transcripts. Reports have shown reciprocal interactions occur between hUCMSCs and macrophages after stimulation with LPS in *vitro*. Soluble factors derived from activated macrophages induce NO production by hUCMSCs in the presence of LPS. Moreover, 3 D hUCMSCs also express a lower level of IFNg to relieve the functional cell apoptosis in response to LPS/CCL_4 stimulation. The responsiveness of hUCMSCs to activating factors is expectable and unavoidable when using these cells for transplantation [42, 43]. In short, the 3 D hUCMSCs demonstrate the advantages of immune-regulation and cell promotion/apoptosis administration, including the effective promotion of M_1/M_2 macrophage switch by secreting an increased antifififibrogenic cytokines, ameliorating proliferation and downregulation of NO of macrophage (Fig. 4D). The scaffolds in 3 D culture probably provided an architectural skeletons in which cell-matrix, cell-cell, and growth factor interactions combine to create regenerative niches [44]. Such 3D systems have been shown to enhance the stem cell functionality and provide greater support for hepatocyte proliferation and functionality than routine 2D culture [45, 46].

3 D hUCMSCs Ameliorate Acute Liver Injury by MAPKs and STAT3 Signaling Pathways

MAPK activation such as p38, JNK, and ERK. MAPK controls the expression of proinflammatory cytokines such as IL-1β, IL-6 and TNF-α, among others [47]. Phosphorylation of p38, JNK, and ERK have also been reported upon stimulation of RAW264.7 cells with Corylin [48], and it could mediate the hyperphosphorylation of Tau molecules [49]. As expected, we could observe that stimulation of RAW264.7 cells with LPS stimulated the phosphorylation of ERK, p38 and JNK. Nevertheless, in the presence of 3 D hUCMSCs, the activation of these MAPKs was significantly prevented. In addition, binding of cytokines to their cognate receptors on the cell surface activates a family of cytoplasmic proteins, designated STATs (signal transducers and activators of transcription), through tyrosine phosphorylation by the receptor-associated Jak kinases. Also, as an important member of STAT family, STAT3 was activated by IL-6 family cytokines and subsequently facilitate tyrosine phosphorylated in response to a variety of stimulus [50]. In this study, we found that decreased STAT3 protein kinases expression in 3 D hUCMSCs, in which the activation of STAT3 was strongly inhibited. In addition, the STAT3 phosphorylation level was inhibited once treated with 3 D hUCMSCs in comparison with the control group (Fig. 4A). These findings proved that the 3 D hUCMSCs and the conditioned medium could alleviate the ALI in mice by a combined strategy of immunoregulation, cell promotion and apoptosis.

Conclusion

In summary, we demonstrated that the 3 D hUCMSCs were more favorable for the ALI therapy compared to 2 D hUCMSCs. Triple regulatory roles of the 3 D hUCMSCs included the effective promotion of M_1/M_2

macrophage switch on the secretion of increased antififibrogenic cytokines, ameliorating proliferation and downregulation of NO of macrophage. The paracrine effect played a key role in ALI repairing. The conditioned medium of 3 D hUCMSCs acted as another potent secretory component containing specific cytokines and small RNAs, which achieved a similar curative effect on ALI. Moreover, the effective suppression of the phosphorylation of extracellular signal-regulated kinases (ERK), c-Jun N-terminal kinases (JNK), the p38 and STAT3 indicated the mitogen-activated protein kinases (MAPKs) and STAT3 signaling pathways. The revelation of the superior moderating effect of 3 D hUCMSCs and the triple regulatory mechanism can open a new route for novel cell-free therapeutics to prevent immune system diseases, which will bring hope to patients with inflammatory and immunologically-mediated diseases.

Abbreviations

MSCs
mesenchymal stem cells
hUCMSCs
human umbilical cord mesenchymal stem cells
3D hUCMSCs
hUCMSCs grown on microcarriers in 3 D suspension culture
3D hUCMSCs©
the conditioned medium of 3 D hUCMSCs
2D hUCMSCs
hUCMSCs grown on 2 D plate. 2D hUCMSCs©:the conditioned medium of 2 D hUCMSCs. ALI:acute liver injury. DMEM:Dulbecco-modifed eagle medium
ELISA
Enzyme-linked immunosorbent assay
qPCR
Quantitative polymerase chain reaction
RT-qPCR
Reverse transcription-quantitative polymerase chain reaction
ELISA
enzyme-linked immunosorbent assay
NO
nitric oxide
iNOS
inducible nitric oxide synthase
LPS
lipopolysaccharide
TNF-α
Tumor necrosis factor alpha
JNK

c-Jun N-terminal kinases
MAPKs
mitogen-activated protein kinases
IL-6
interleukin-6
IL-1β
interleukin-1β
ERK
extracellular signal-regulated kinases
(TLR)-4
Toll-like receptor.

Declarations

Supplementary Information

The online version contains supplementary material available at xxx.

Acknowledgement

We would like to acknowledge the reviewers for their helpful comments on this paper. And the authors extend their appreciation to the Researchers Supporting Project of Junshi Biosciences Company, Shanghai, China.

Funding

Not applicable.

Author Contributions

This study was designed and performed by JHZ &JQZ with help YP, YL, and AM. The paper was written and revised by JHZ, AM, MG and YZ. JHZ &JQZ contributed equally.

Data Availability Statement

The data that support the findings of this study are available from the corresponding author upon reasonable request.

Ethics approval and consent to participate

All experiments were approved by the Ethics Committee of the National Academy of science and implemented as per the guidelines established by the Ministry of Health of People's Republic of China. The study protocol were conducted in conformity with the institutional guidelines for the care and use of laboratory animals in East China University of Science and technology, and also with the National

Institutes of Health Guide for Care and Use of Laboratory Animals (Publication No. 85-23, revised 1985). hucMSCs were obtained as a kind gift from Prof. Huiming Xu at Renji Hospital, School of Medicine, Shanghai Jiaotong University.

Consent for publication

Not applicable.

Competing interests

All authors declare no conflicts of interest.

Author details

[1]State Key Laboratory of Bioreactor Engineering, East China University of Science and Technology, Shanghai 200237, People's Republic of China.

References

1. Effenberger M, Grander C, Grabherr F, Griesmacher A, Ploner T, Hartig F, et al. Systemic inflammation as fuel for acute liver injury in COVID-19. Digest Liver Dis. 2021; 53(2): 158-65.
2. Medzhitov R. Origin and physiological roles of inflammation. Nature 2008; 454(7203): 428-35.
3. Huang ZF, Massey JB, Via DP. Differential regulation of cyclooxygenase-2 (COX-2) mRNA stability by interleukin-1β (IL-1β) and tumor necrosis factor-α (TNF-α) in human in vitro differentiated macrophages. Biochem Pharmacol. 2000; 59(2): 187-94.
4. Gaibani P, Caroli F, Nucci C, Sambri V. Major surface protein complex of Treponema denticola induces the production of tumor necrosis factor α, interleukin-1β, interleukin-6 and matrix metalloproteinase 9 by primary human peripheral blood monocytes. J Periodontal Res. 2010; 45(3): 361-66.
5. Krasnodembskaya A, Song Y, Fang X, Gupta N, Serikov V, Lee JW, et al. Antibacterial Effect of Human Mesenchymal Stem Cells Is Mediated in Part from Secretion of the Antimicrobial Peptide LL-37. Stem Cells 2010; 28(12): 2229-38.
6. Ouchi N, Parker JL, Lugus JJ, Walsh K. Adipokines in inflammation and metabolic disease. Nat Rev Immunol. 2011; 11(2): 85-97.
7. Greten FR, Grivennikov SI. Inflammation and Cancer: Triggers, Mechanisms, and Consequences. Immunity 2019; 51(1): 27-41.
8. Welty-Wolf KE, Carraway MS, Ortel TL, Piantadosi CA. Coagulation and inflammation in acute lung injury. Thromb Haemostasis. 2002; 88(1): 17-25.
9. Hotamisligil GS. Inflammation and metabolic disorders. Nature 2006; 444(7121): 860-67.
10. Wisse BE. The Inflammatory Syndrome: The Role of Adipose Tissue Cytokines in Metabolic Disorders Linked to Obesity. J Am Soc Nephrol. 2004; 15(11): 2792-00.

11. Mattson MP, Barger SW, Furukawa K, Bruce AJ, Wyss CT, Mark RJ, et al. Cellular signaling roles of TGFβ, TNFα and βAPP in brain injury responses and Alzheimer's disease. Brain Res Rev. 1997; 23(1): 47-61.
12. Park D, Spencer JA, Koh BI, Kobayashi T, Fujisaki J, Clemens TL, et al. Endogenous Bone Marrow MSCs Are Dynamic, Fate-Restricted Participants in Bone Maintenance and Regeneration, Cell Stem Cell 2012; 10(3): 259-72.
13. Li C, Wu X, Tong J, Yang X, Zhao J, Zheng Q, et al. Comparative analysis of human mesenchymal stem cells from bone marrow and adipose tissue under xeno-free conditions for cell therapy, Stem Cell Res Ther. 2015; 6(1): 55.
14. Qi Y, Ma J, Li S, Liu W. Applicability of adipose-derived mesenchymal stem cells in treatment of patients with type 2 diabetes. Stem Cell Res Ther. 2019; 10(1): 274.
15. Ishikawa T, Banas A, Hagiwara K, Iwaguro H, Ochiya T. Stem Cells for Hepatic Regeneration: The Role of Adipose Tissue Derived Mesenchymal Stem Cells. Curr Stem Cell Res T. 2010; 5(2): 182-89.
16. Galipeau J, Sensébé L. Mesenchymal Stromal Cells: Clinical Challenges and Therapeutic Opportunities. Cell Stem Cell 2018; 22(6): 824-33.
17. El-Badri NS, Maheshwari A, Sanberg, PR. Mesenchymal Stem Cells in Autoimmune Disease, Stem Cells Dev. 2004; 13(5): 463-72.
18. Meng F, Xu R, Wang S, Xu Z, Zhang C, Li, Y, et al. Human umbilical cord-derived mesenchymal stem cell therapy in patients with COVID-19: a phase 1 clinical trial. Signal Transduct Tar. 2020; 5(1): 172.
19. Kavianpour M, Saleh M, Verdi J. The role of mesenchymal stromal cells in immune modulation of COVID-19: focus on cytokine storm. Stem Cell Res Ther. 2020; 11(1): 404.
20. Uccelli A, Moretta L, Pistoia V. Mesenchymal stem cells in health and disease. Nat Rev Immunol. 2008; 8(9): 726-36.
21. Jaimes Y, Naaldijk Y, Wenk K, Leovsky C, Emmrich F. Mesenchymal Stem Cell-Derived Microvesicles Modulate Lipopolysaccharides-Induced Inflammatory Responses to Microglia Cells. Stem Cells. 2017; 35(3): 812-23.
22. Pittenger MF, Mackay AM, Beck SC.,Jaiswal RK, Douglas R, Mosca JD, et al. Multilineage Potential of Adult Human Mesenchymal Stem Cells. Science 1999; 284(5411): 143-47.
23. Shi Y, Wang Y, Li Q, Liu K, Hou J, Shao C, et al. Immunoregulatory mechanisms of mesenchymal stem and stromal cells in inflammatory diseases.Nat Rev Nephrol. 2018; 14(8): 493-07.
24. Salem HK, Thiemermann C. Mesenchymal Stromal Cells: Current Understanding and Clinical Status. Stem Cells 2010; 28(3): 585-96.
25. Bieback K, Kern S, Kluter H, Eichler H. Critical parameters for the isolation of mesenchymal stem cells from umbilical cord blood. Stem Cells 2004; 22(4): 625-34.
26. Kumar P, Nagarajan A, Uchil PD. Analysis of Cell Viability by the MTT Assay. Cold Spring Harb Protoc. 2018; 2018(6), https://doi.org/10.1101/pdb.prot095505.

27. Zhou Z, Yin Y, Chang Q, Sun G, Lin J, Dai Y. Downregulation of B-myb promotes senescence via the ROS-mediated p53/p21 pathway, in vascular endothelial cells. Cell Proliferat. 2017; 50(2): 12319.
28. Friedman R, Betancur M, Boissel L, Tuncer H, Cetrulo C, Klingemann Hans. Umbilical Cord Mesenchymal Stem Cells: Adjuvants for Human Cell Transplantation. Biol Blood Marrow Tr. 2007; 13(12): 1477-86.
29. Majore I, Moretti P, Stahl F, Hass R, Kasper C. Growth and Differentiation Properties of Mesenchymal Stromal Cell Populations Derived from Whole Human Umbilical Cord. Stem Cell Rev Rep. 2011; 7(1): 17-31.
30. Xie Z, Wang Y, Huang J, Qian N, Shen G, Chen L. Anti-inflammatory activity of polysaccharides from Phellinus linteus by regulating the NF-κB translocation in LPS-stimulated RAW264.7 macrophages. Int J Biol Macro. 2019; 12961-67.
31. Sasajima H, Miyagi S, Yamada S Kakizaki Y, Kamei T, Unno M, et al. Cytoprotective Effects of Mesenchymal Stem Cells During Liver Transplantation From Donors After Cardiac Death in Swine. Transpl P. 2020; 52(6): 1891-00.
32. Rocheteau P, Chatre L, Briand D, Mebarki M, Jouvion G, Bardon J, et al. Sepsis induces long-term metabolic and mitochondrial muscle stem cell dysfunction amenable by mesenchymal stem cell therapy. Nat Commun. 2015; 6(1): 10145.
33. Xu W, Liu LZ, Loizidou M, Ahmed M, Charles IG. The role of nitric oxide in cancer, Cell Res. 2002; 12(5): 311-20.
34. Liberatore GT, Jackson-Lewis V, Vukosavic S, Mandir AS, Vila M, McAuliffe, WG, et al. Inducible nitric oxide synthase stimulates dopaminergic neurodegeneration in the MPTP model of Parkinson disease. Nat Med. 1999; 5(12): 1403-09.
35. Cinelli MA, Do HT, Miley GP, Silverman RB. Inducible nitric oxide synthase: Regulation, structure, and inhibition. Med Res Rev. 2020; 40(1): 158-89.
36. Possel H, Noack H, Putzke J, Wolf G, Sies H. Selective upregulation of inducible nitric oxide synthase (iNOS) by lipopolysaccharide (LPS) and cytokines in microglia: In vitro and in vivo studies, Glia 2000; 32(1): 51-59.
37. HEINRICH PC. BEHRMANN I, HAAN S, HERMANNS HM. MÜLLER-NEWEN G, SCHAPER F. Principles of interleukin (IL)-6-type cytokine signalling and its regulation. Biochem J. 2003; 374(1): 1-20.
38. Judd LM, Bredin K, Kalantzis A, Jenkins BJ, Ernst M, Giraud AS. STAT3 Activation Regulates Growth, Inflammation, and Vascularization in a Mouse Model of Gastric Tumorigenesis. Gastroenterology 2006; 131(4): 1073-85.
39. Zhou Y, Cheng Z, Wu Yin, Wu Q, Liao X, Zhao Y, et al. Mesenchymal stem cell–derived conditioned medium attenuate angiotensin II-induced aortic aneurysm growth by modulating macrophage polarization. J Cell Mol Med. 2019; 23(12): 8233-45.
40. Ren J, Su D, Li L, Cai H, Zhang M, Zhai J, et al. Anti-inflammatory effects of Aureusidin in LPS-stimulated RAW264.7 macrophages via suppressing NF-κB and activating ROS- and MAPKs-dependent Nrf2/HO-1 signaling pathways. Toxicolo Appl Pharm. 2020; 387: 114846.

41. Ra JC, Kang SK, Shin IS, Park HG, Joo SA, Kim JG, et al. Stem cell treatment for patients with autoimmune disease by systemic infusion of culture-expanded autologous adipose tissue derived mesenchymal stem cells. J Transl Med. 2011; 9(1): 181.
42. Herberts CA, Kwa Marcel SG, Hermsen Harm PH. Risk factors in the development of stem cell therapy. J Transl Med. 2011; 9(1): 29.
43. Casiraghi F, Remuzzi G, Abbate M, Perico N. Multipotent Mesenchymal Stromal Cell Therapy and Risk of Malignancies. Stem Cell Rev Rep. 2013; 9(1): 65-79.
44. Sokolsky-Papkov M, Agashi K, Olaye A, Shakesheff K, Domb AJ. Polymer carriers for drug delivery in tissue engineering. Adv Drug Deliv Rev. 2007; 59(4): 187-06.
45. Elkayam T, Amitay-Shaprut S, Dvir-Ginzberg M, Harel T, Cohen S. Enhancing the Drug Metabolism Activities of C3A— A Human Hepatocyte Cell Line—By Tissue Engineering Within Alginate Scaffolds. Tissue Eng. 2006; 12(5): 1357-68.
46. Cheng N., Wauthier E, Reid LM. Mature human hepatocytes from ex vivo differentiation of alginate-encapsulated hepatoblasts. Tissue Eng Pt A. 2008; 14(1): 1-7.
47. Gorina R, Font-Nieves M, Márquez-Kisinousky L, Santalucia T, Planas AM. Astrocyte TLR4 activation induces a proinflammatory environment through the interplay between MyD88-dependent NFκB signaling, MAPK, and Jak1/Stat1 pathways. Glia 2011; 59(2): 242-55.
48. Hung Y, Fang, S, Wang, S, Cheng W, Liu P, Su C, et al. Corylin protects LPS-induced sepsis and attenuates LPS-induced inflammatory response, Sci Rep. 2017; 7(1): 46299.
49. Kim EK, C EJ Pathological roles of MAPK signaling pathways in human diseases, BBA - Mol Basis Dis. 2010; 1802(4): 396-05.
50. Akira S, Nishio Y, Inoue M, Wang X, We S, Matsusaka T, et al. Molecular cloning of APRF, a novel IFN-stimulated gene factor 3 p91-related transcription factor involved in the gp130-mediated signaling pathway, Cell 1994; 77(1): 63-71.

Scheme

Scheme 1 is available in Supplemental Files section.

Figures

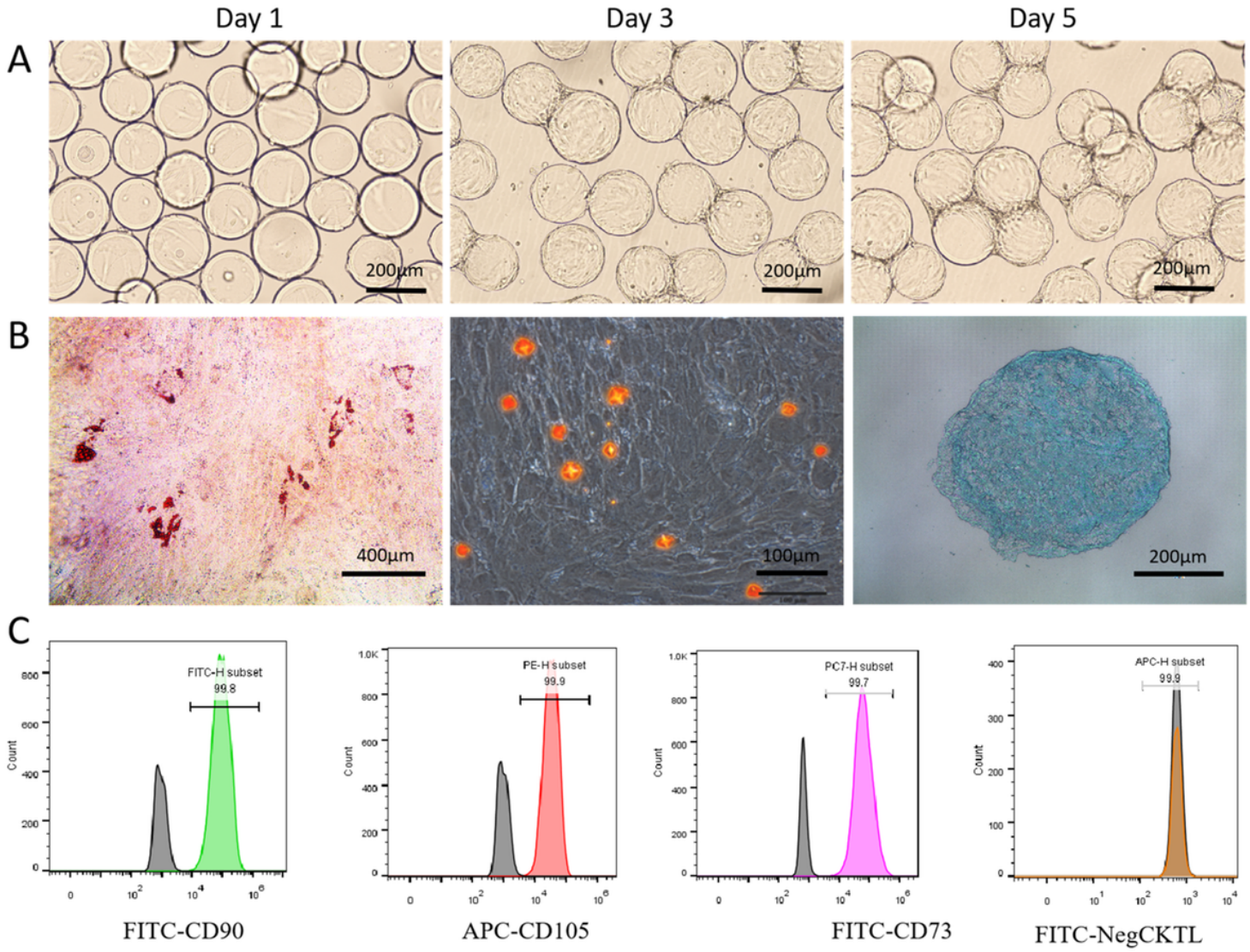

Figure 1

(A) Morphology and distribution of cells on microcarriers at different time points (Day 1, Day 3 and Day 5) cultured by 1.5 L bioreactor. (B) Adipogenic, osteogenic and chondrogenic differentiation of hUCMSCs. Oil Red O staining of adipogenic differentiation (scale bar: 400 um). Alizarin red staining of osteogenic differentiation (scale bar: 100 um). Alcian Blue staining of chondrogenic differentiation (scale bar: 200 um). (C) Characterization of expensing hUCMSCs surface markers by flow cytometry using positive markers (FITC CD90, APC CD105 and FITC CD73) and negative ones (FITC CD14, CD19, CD34, CD45 and HLA-DR).

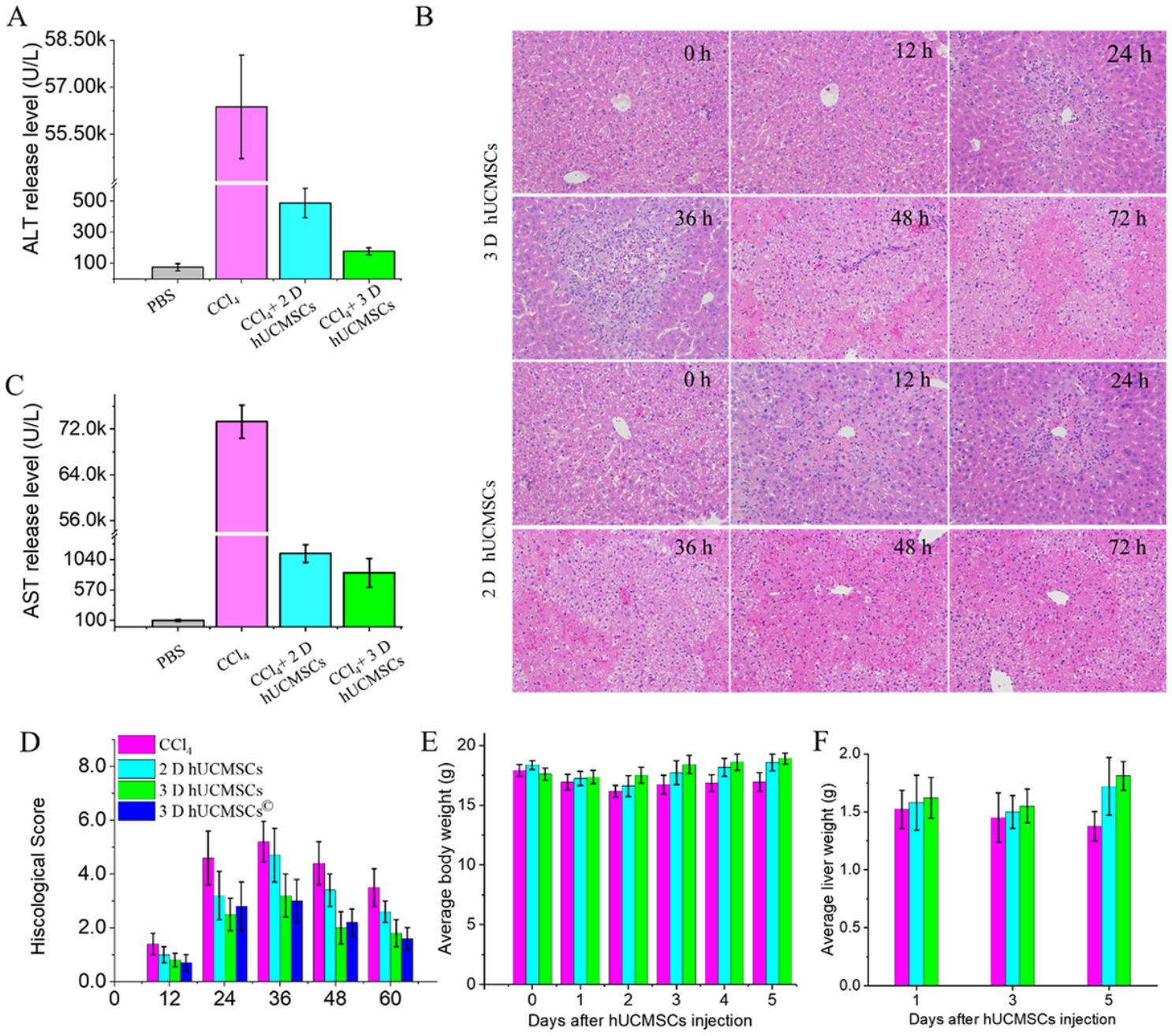

Figure 2

hUCMSCs pretreatment attenuates acute liver injury in mice. A. Time course of ALT serum levels. B. Representative histopathological images of H&E-stained liver sections from CCl_4-treated mice pretreated with the hUCMSCs. C Time course of AST serum levels. D. Histological scores for liver sections. E. Average body weight of ALI mice after treatment with hUCMSCs or conditioned medium. F. Average liver weight of ALI mice after treatment with hUCMSCs.

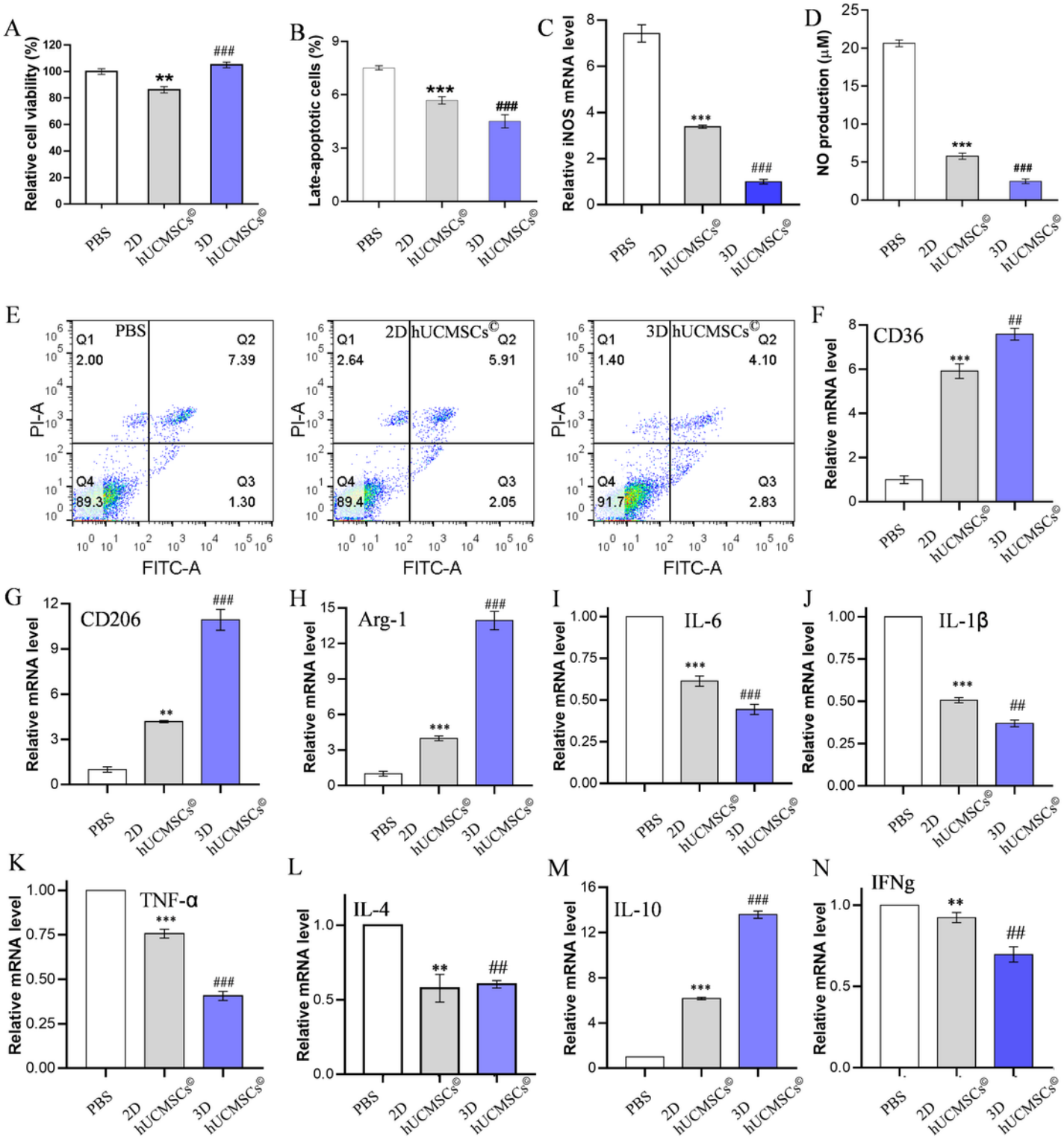

Figure 3

(A) Cell viability of the conditioned medium using RAW 264.7 as model cell. (B) Late apoptotic cell percentages of RAW 264.7 cells when treated with the 2D hUCMSCs© and 3D hUCMSCs©. (C&D) Relative iNOS mRNA level and NO production. (E) Flow cytometry of RAW 264.7 cells. (F-N) Serum cytokines levels of ALI mice when treated with PBS buffer or the conditioned medium. Bar graphs represent means ± SD

(n = 3 per group). **p < 0.01, ***p < 0.001 vs. control group; ##p < 0.01, ###p < 0.001 vs. LPS group. Arg-1: Arginase-1; IL: interleukin, TNF-α: tumor necrosis factor alpha; iNOS: inducible nitric oxide synthase.

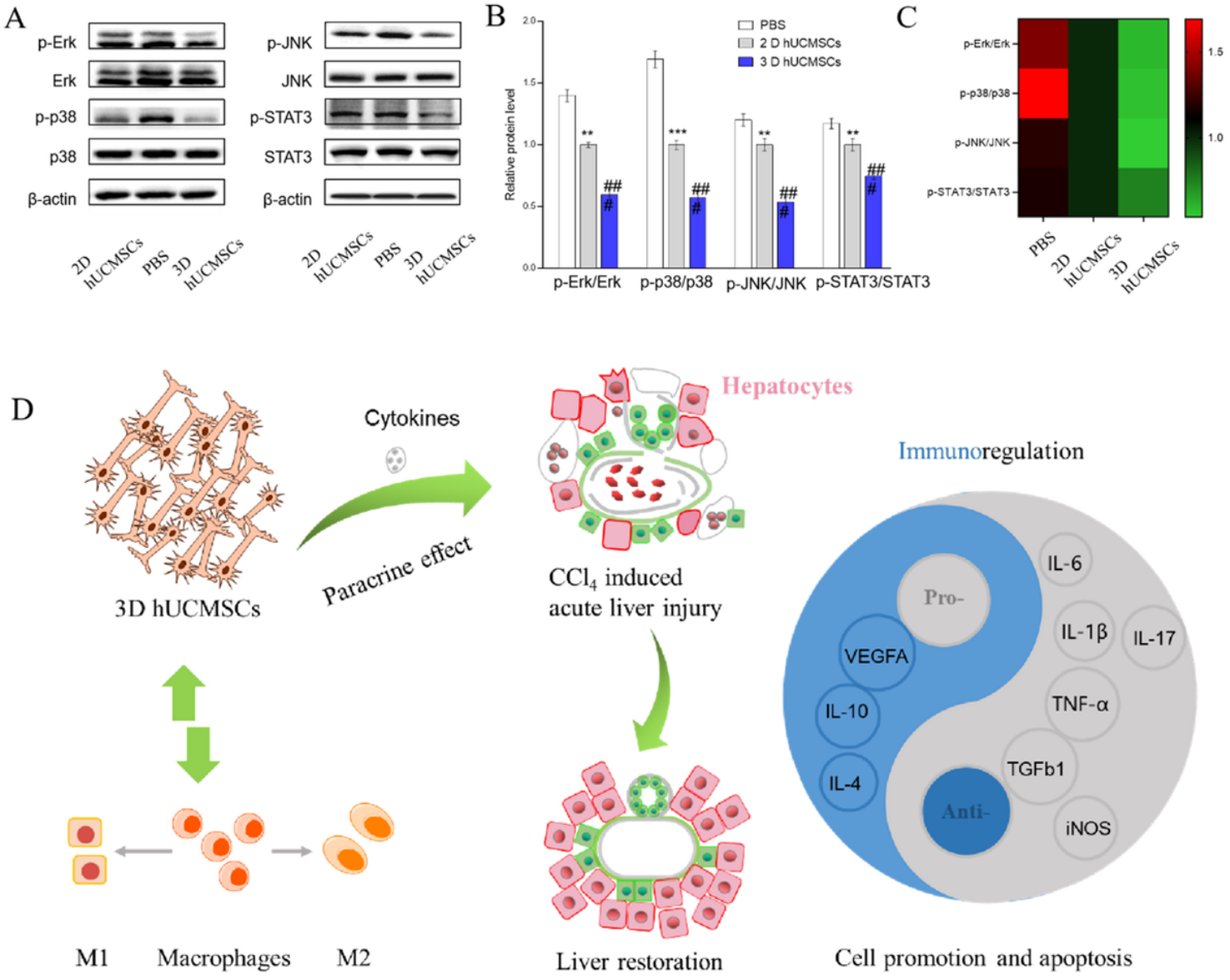

Figure 4

(A) Western blotting analysis of the protein expression in the liver tissue of ALI mice treated with the PBS or conditioned medium. (B) Serum protein levels in ALI mice at 24 h and the heat-map analysis of relative protein expression of key factors of MAPKs and STAT3 signaling pathways by western blot. (D) Proposed mechanisms of hUCMSCs action in liver restoration. CCL_4 destroys hepatocytes and causes detrimental cytokines, further damaging liver tissue. Implanted hUCMSCs respond to the signals and proliferate and transdifferentiate to repair the liver tissue. Through paracrine effects, the hUCMSCs also induce the expression of cytokines in the host. These cytokines are involved in immunoregulation and cells proliferation, and apoptosis. *p < 0.05 *vs.* control group, **p < 0.01 *vs.* control group, ***p < 0.001 *vs.* control group; ##p < 0.01, ###p < 0.001 *vs.* LPS group.

Supplementary Files

This is a list of supplementary files associated with this preprint. Click to download.

- Scheme1.tif
- Supplementarymaterials.docx